ISSN 1330–0016
CODEN FIZBE7

HOW TO PROBE THE DYNAMICS OF THE FIREBALL EXPANSION?

MIHAI PETROVICI

National Institute for Physics and Nuclear Engineering, Bucharest, Romania

Paper devoted to honour the memory of Professor Nikola Cindro

Received 26 June 2003; revised manuscript received 29 October 2003
Accepted 8 December 2003 Online 3 March 2004

Model predictions on the yield distributions for different reaction products and on the collective energy of the expanding fireball as a function of break-up time, corroborated with the experimental results on the small-angle two-particle longitudinal correlation functions, transition energy dependence as a function of transversal momentum and azimuthal distributions of the collective expansion, evidence in a clear way the possibility to access different time slots in the dynamics of the fireball.

PACS numbers: 25.75.Ld, 25.70.Pq UDC 539.17

Keywords: heavy ions, expansion, clustering, emission time, small angle correlations, transition energy, mean kinetic and flow energy azimuthal distributions

1. *Introduction*

Detailed exclusive experimental information from highly central and mid-central relativistic heavy ion collisions has been obtained in the last two decades. However, one of the main question, related to the possibility of extracting information on the nuclear equation of state, which motivated this field of research, has not yet been answered. The search for hot and dense nuclear matter created in heavy-ion collisions is a delicate task, dynamical aspects and finite size effects playing an important role. Obviously it is necessary to pin down the dynamical consequences of high incident energy necessary to reach the high temperature and pressure and the possibility to reach thermal equilibrium in finite systems created in such collisions. Equally important is to understand dynamical aspects related to the evolution stage of the formed fireball. Thus, detailed experimental information on the expansion dynamics is required in order to get higher sensitivity to the equation of state.

At first look, based on azimuthal symmetry and negligible spectator nuclear-

matter arguments, highly central heavy-ion collisions seem to deliver the less biased information on the fireball dynamics.

Indeed, as it was predicted in early seventies [1, 2], the collective expansion of hot and dense nuclear matter produced in such collisions was evidenced experimentally [3–11].

However, two aspects are worth mentioning:

- Although the axial symmetry of the dynamical evolution holds for highly central collisions, the spherical one has to be carefully studied. Preequilibrium emission, corona and transparency effects influence the conclusion on the spheroidal symmetry of the expanding object, large deviations from spherical expansion being observed [9,12–14].
- As the nuclear matter can escape freely in any direction perpendicular to the collision axis, starting from the very first moment of the collision, the confinement is realized only by the regions of nuclei which did not yet enter into the reaction zone along the collision direction.

Recently, small angle correlation studies from central heavy ion collisions [15] have shown the possibility to gain insight into the emission times for different reaction products and size of the emission source, confirming the model predictions [7].

For mid-central collisions, one has to deal with rotating expanding objects in the presence of the spectator matter which, apparently, is rather complex. A closer examination shows that there are also some advantages in studying such type of collisions:

- the centrality can be used to control the shape and content of the fireball and shadowing matter,
- for a given centrality, the passage time of the shadowing objects can be controlled varying the incident energy,
- the confinement of the fireball by the spectators is more compact in the reaction plane
- rotation and shadowing can be used as internal clocks for getting deeper information on the expansion dynamics.

The preferential emission of fragments perpendicular to the reaction plane, called "squeeze-out" phenomena, initially predicted by hydrodynamical calculations [16] has been extensively studied experimentally [17–25].

Although this phenomenon was studied in detail as a function of centrality, type of emitted particle, transverse momentum and mass of the colliding systems, these studies have recently focussed on the azimuthal distribution of the momentum [23] or energy [12, 13, 26, 27].

In this contribution, we analyze the predictions of a hybrid model [7] in terms of yield distributions for different reaction products and on the collective energy of

the expanding fireball as a function of break-up time. Comparison of the model predictions with the experimental results on the small angle two-particle longitudinal correlation functions, transition energy as a function of transverse momentum for different reaction products and azimuthal distributions of the collective expansion clearly evidence the possibility to access different exposure times in the dynamics of the fireball expansion.

2. Model predictions on the yield distributions as a function of break-up time and transverse momentum

The model considers an isotropic expansion described by semianalytical solutions of a hydrodynamical model for an ideal nucleonic gas and the clustering by a statistical disassembly [7]. The break-up condition is based not on a global equilibrium assumption but on a geometrical concept [28]. A Coulomb expansion after breakup was introduced, considering that particles with charge Z_{IMF} feel the Coulomb repulsion of a source with fireball charge, Z_{FB} [12]. The recoil effects have been neglected in the present stage of the model. Simple analytical solutions for the isentropic expansion of a spherical ideal nucleonic gas can be worked out for a self-similar expansion. This hypothesis is supported by the transport model calculations which show that the expansion velocity within a good approximation is proportional to the distance to the symmetry center during the expansion process. The model has three parameters: the density in the center of the fireball at the initial moment, a parameter related to the shape of the initial density distribution and a break-up parameter which takes into account the difference due to a mixed composition relative to the monoatomic one for which the geometrical concept of break-up moment can be worked out analytically. These parameters are fixed once they have been adjusted in order to obtain the best reproduction of the experimental results for a given reaction product. Taking into account the scope of the present work, we will describe mainly qualitative aspects of the model predictions. Using the parameters reported in Ref. [7] for 250 A MeV, we calculated the yield of different reaction products as a function of break-up time, t_b and normalized transverse momentum per nucleon to the projectile momentum per nucleon in the c.m. system, $p_t^{(0)} = (p_t/A)/(p_P^{\mathrm{cm}}/A_P)$ (A is the mass of the corresponding reaction product and A_P is the projectile mass). The results for p, d, ^{4}He and Li fragments, for a fireball characterized by 200 participating nucleons, A_{part}=200 and N/Z corresponding to 250 A MeV Au + Au collision at an impact parameter of about 5 fm, can be followed in Fig. 1.

Already from such representations, one can easily conclude that large differences in the production yield as a function of break-up time between different species appear in the region of low transverse momenta, heavier fragments being produced on the average at larger values of the break-up time relative to the light particles. For $p_t^{(0)} > 0.8$, for most products, the maximum of the distribution is localized at the same value of t_b.

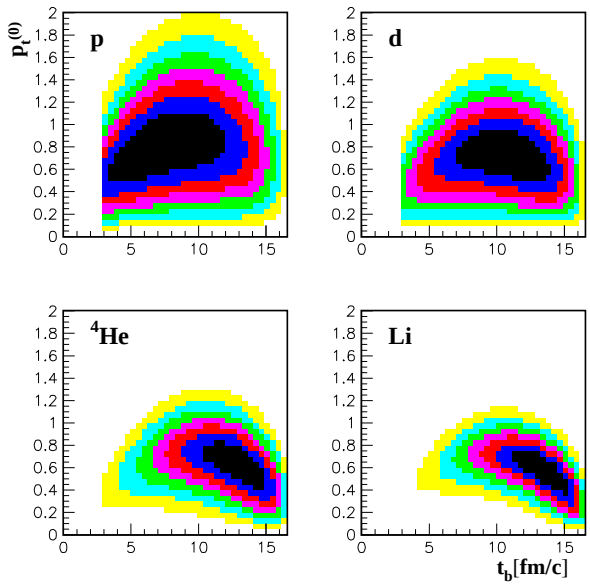

Fig. 1. Production probability for p, d, ^{4}He *and* ^{7}Li *as a function of* $p_t^{(\circ)}$ *and* t_b, *estimated by the hybrid model for an* $A_{\rm part} = 200$ *fireball and 250 A* MeV *incident energy* Au + Au.

These trends can be followed much easier in Figs. 2, 3 and 4, where the production yields for p, d, ^{4}He and Li fragments are represented as a functions of t_b for three regions of $p_t^{(0)}$, $0.2 < p_t^{(0)} < 0.4$, $0.8 < p_t^{(0)} < 1.0$ and $1.4 < p_t^{(0)} < 1.6$.

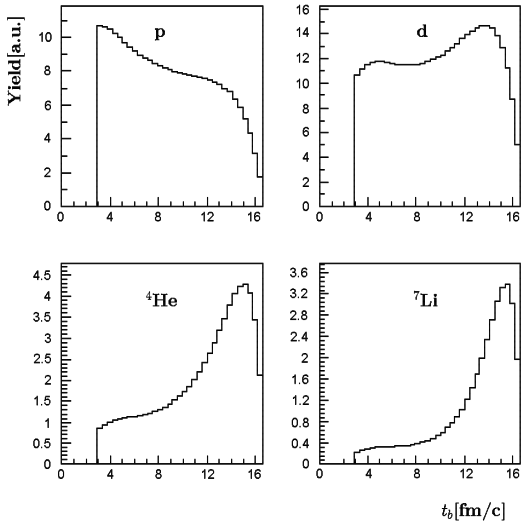

Fig. 2. Yield distributions for p, d, ^{4}He *and* ^{7}Li *as a function of* t_b, *for* $0.2 \le p_t^{(\circ)} \le 0.4$, $A_{\rm part} = 200$ *and 250 A* MeV *incident energy* Au + Au.

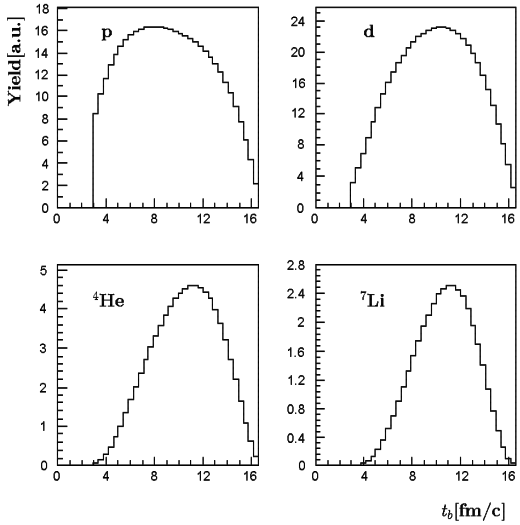

Fig. 3. Yield distributions for p, d, ^{4}He *and* ^{7}Li *as a function of* t_b*, for* $0.8 \leq p_t^{(\circ)} \leq 1.0$*,* $A_{\rm part} = 200$ *and 250 A* MeV *incident energy* Au + Au.

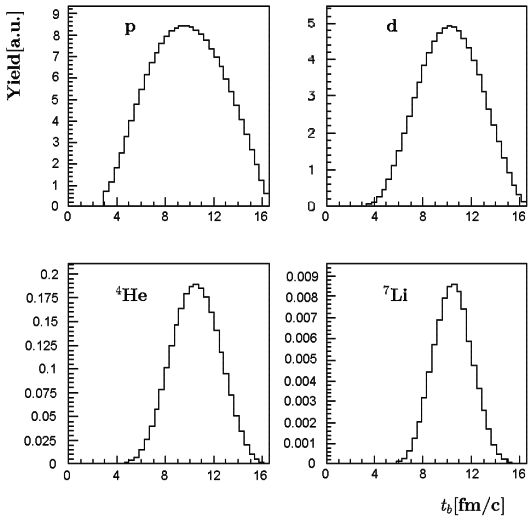

Fig. 4. Yield distributions for p, d, ^{4}He *and* ^{7}Li *as a function of* t_b*, for* $1.4 \leq p_t^{(\circ)} \leq 1.6$*,* $A_{\rm part} = 200$ *and 250 A* MeV *incident energy* Au + Au.

At low transverse momenta, Fig. 2, protons are produced during the whole expansion process, with a maximum at the beginning of the process, the deuterons have almost a mirrored distribution relative to the protons, and complex fragments are produced mainly towards the end of the expansion when the fireball is charac-

terized by a lower expansion, lower density and lower temperature [7].

This trend is drastically reduced at $0.8 < p_t^{(0)} < 1.0$ (see Fig. 3) and disappears completely at high values of $p_t^{(0)}$, namely at $1.4 < p_t^{(0)} < 1.6$ (see Fig. 4), where the yield distributions for the four species have maxima at the same value of t_b. Besides the obvious difference in the relative yield, the breaking-time widths are still different, narrower time distributions being characteristic for complex fragments.

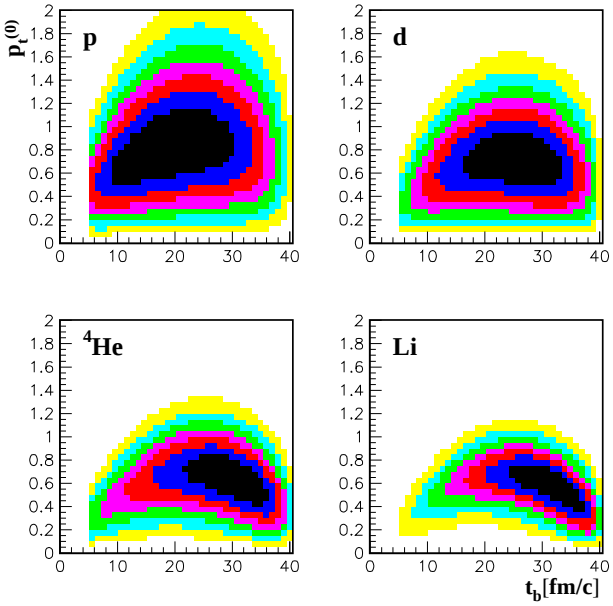

Fig. 5. Production probability for p, d, ^{4}He *and* ^{7}Li *as a function of* $p_t^{(\circ)}$ *and* t_b, *estimated by the hybrid model for a* $A_{\rm part}$ *= 200 fireball and 90* A MeV *incident energy.*

Similar trends are observed at other incident energies. The results for 90 A MeV and $A_{\rm part}$=200 can be followed in Fig. 5.

3. Model predictions on the mean kinetic energies and collective expansion as a function of break-up time and azimuth

In the previous section, it is shown that imposing conditions on the transverse momenta one could evidence differences, or similarities, in the time when different species are emitted by an expanding object. How such differences can be evidenced experimentally will be shown in Sect. 4.

Now we concentrate on the kinetic energy distributions and on the collective energy extracted from them. Since the advent of the 4π geometry experimental devices, complete energy spectra for most of the reaction products became available. A two-dimensional representation of the reaction-product yields as a function of

break-up time and kinetic energy per nucleon, $E_{\rm kin}/A_{\rm IMF}$, is presented in Fig. 6. Qualitatively, they present the same trends as those observed in the previous representations in terms of $p_t^{(0)}$.

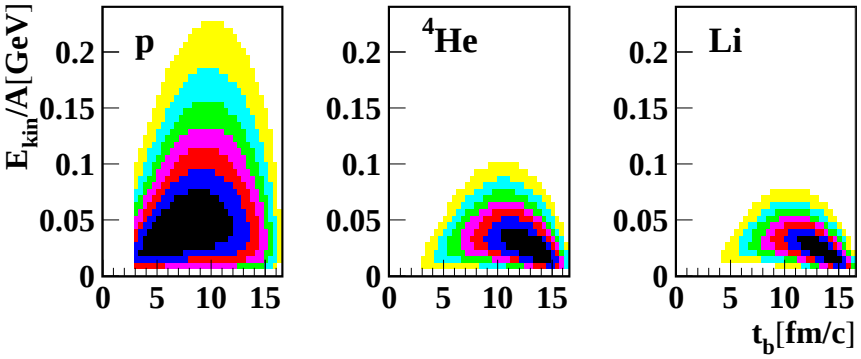

Fig. 6. Two dimensional representations of the production probability for p, ^{4}He *and* ^{7}Li *as a function of* $E_{\rm kin}/A_{\rm IMF}$ *and* t_b*, predicted by the hybrid model for a* $A_{\rm part} = 200$ *nucleons fireball populated in* Au + Au *collision at 250 A* MeV.

Let's take one of the reaction products, ^{4}He, integrate the corresponding two-dimensional representation on the break-up time from different initial values of the break-up time, $t_b^{\rm min}$, until the total expansion time, project the result on the $E_{\rm kin}/A_{\rm IMF}$ axis and find the corresponding $< E_{\rm kin} >$ value. The result of this analysis is presented in Fig. 7.

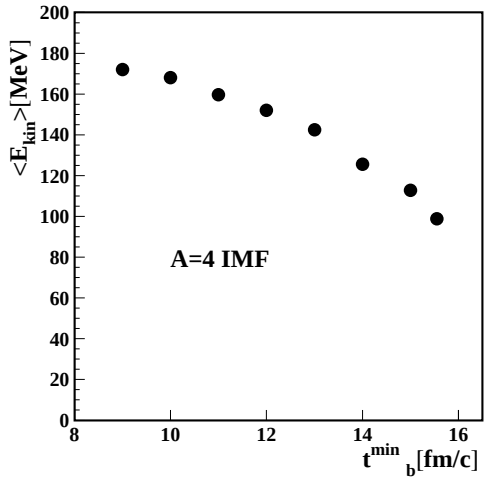

Fig. 7. Average kinetic energy of the ^{4}He *fragments emitted by the fireball during its expansion later than* $t_b^{\rm min}$.

It is seen that the energy spectra accumulated during the exposure times which started later in the expansion process are characterized by lower $< E_{\rm kin} >$ values

relative to those accumulated with larger exposure times, i.e., earlier t_b^{min}. Such trend is characteristic for all species, and intermediate mass fragments show a stronger dependence on t_b^{min} relative to the light particles.

This can be easily followed in Fig. 8 where the mean kinetic energies of different reaction products as a function of their mass, are shown for three different time slots.

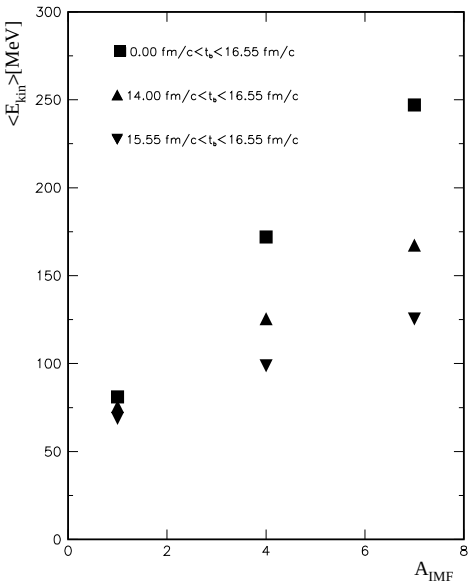

Fig. 8. Mean kinetic energy of Z=1, 2 and 3 fragments as a function of their most probable mass, for three different slots in the break-up time.

The natural question is how to access such information in a real experiment? Let's consider a given collision geometry, as the one presented in Fig. 9. One can

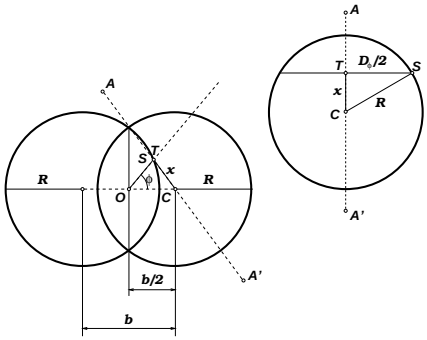

Fig. 9. Geometric representation of the collision geometry used for calculating $D_\phi/2$ as a function of azimuth ϕ defined by the point T on the border of the fireball. The insert on the right sketches the cut of the right nucleus crossing its center C and the point T and which is parallel to the collision axis. Distance $D_\phi/2$ measures the time after which spectators cease to screen the fireball matter.

calculate easily the $D_\phi/2$ value with which two (spectator) nuclei move apart from the collision zone, after the system reached the maximum overlap, such that an observer, placed in the plane crossing the center of mass O, orthogonal to the collision axis, at azimuth ϕ, observes directly the center of the fireball O.

The azimuthal dependence of $D_\phi/2$ can be followed in Fig. 10. Thus, for a given incident energy, one can calculate the corresponding times. Starting from this moment until the end of the process, the observer could have a direct view on the fireball evolution, not hindered by the presence of the spectators.

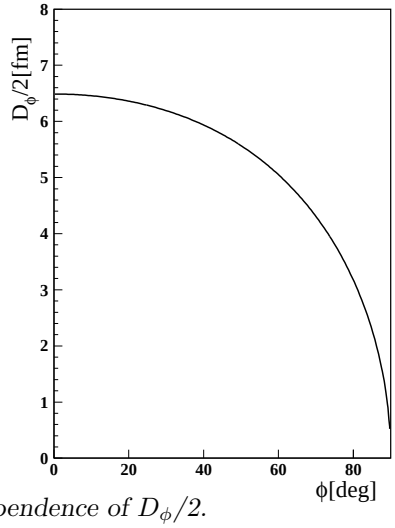

Fig. 10. Azimuthal dependence of $D_\phi/2$.

Using the simple assumption that at the moment of maximum overlap of the colliding nuclei, the evolution of the formed fireball is in the middle of the expansion process, it is rather simple, using the information presented above, to calculate the mean kinetic energies of the reaction products as a function of azimuth ϕ. Whenever one deals with a thermal motion superimposed upon a collective velocity field, the mean kinetic energy can be written within the nonrelativistic approximation as

$$\langle E_{\rm kin}^{\rm cm} \rangle \approx \frac{1}{2} A\, m_0 < \beta_{\rm flow}^2 > + \frac{3}{2} \text{“}T\text{”} \,. \tag{1}$$

Fitting the mean kinetic energy as a function of mass by such an expression for different azimuthal angles, the flow energy per nucleon $E_{\rm coll}$ and the “temperature” “T” are obtained (non-explicit treatment of the Coulomb contribution results in systematically overestimated values of the real temperature T [8]). In Eq. (1), A is the fragment mass number and m_0 is the nucleon rest mass.

The results of an analysis, following the recipe presented above, for Au + Au collision at 250 A MeV and $A_{\rm part}$=200 nucleons, are shown in Fig. 11.

Although the present model calculations do not consider important effects related to the collision dynamics or preequilibrium processes, a remarkable agreement

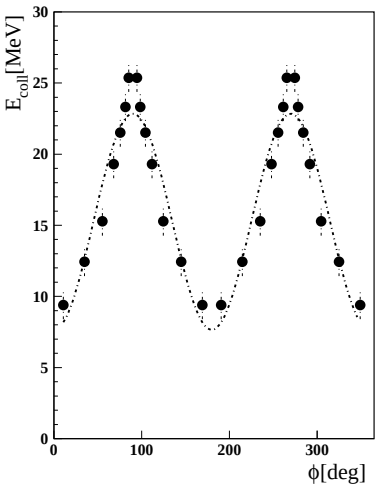

Fig. 11. Azimuthal dependence of the collective energy predicted by the hybrid model presented in the text, for Au + Au *collision at 250 A* MeV *and a collision geometry characterized by* $A_{\rm part}$*=200 nucleons, ∼5* fm *impact parameter.*

between these results and experimental observations, presented in the next section, is observed.

This confirms the possibility to access detailed information on the expansion process as a function of time, performing experimental studies on the azimuthal distribution of mean kinetic and collective energies.

4. Experimental confirmations of the model predictions

This section presents some experimental results which confirm the conclusions of the previous sections, based on the results of model calculations.

As it was mentioned in the Introduction, a nice experimental analysis based on small-angle correlations of pairs of nonidentical reaction species was performed for ^{96}Ru(^{96}Zr) + ^{96}Ru(^{96}Zr) central collisions [15]. If $Y_{12}(\vec{p}_1, \vec{p}_2)$ is the coincidence yield of pairs having momenta $\vec{p}_1$ and $\vec{p}_2$, the two-particle correlation function can be written as:

$$1 + R(\vec{p}_1, \vec{p}_2) = \mathcal{N} \frac{\sum\limits_{\rm events,pairs} Y_{12}(\vec{p}_1, \vec{p}_2)}{\sum_{\rm events,pairs} Y_{12,\rm mix}(\vec{p}_1, \vec{p}_2)} \,. \tag{2}$$

where the subscript "mix" means taking particle 1 and particle 2 from different events. $\mathcal{N}$ is a normalization factor.

The correlation function is projected on the relative momentum $\vec{q}$:

$$\vec{q} = \mu \vec{v}_{12} = \mu(\vec{v}_1^{\,\rm cm} - \vec{v}_2^{\,\rm cm}) \,. \tag{3}$$

$\vec{v}_i^{\,\rm cm}$ are velocities of the two particles in the center of mass of the interacting nuclei and $\mu = m_1 m_2/(m_1 + m_2)$ is the reduced mass of the corresponding pair. If one

considers the angle ζ between $\vec{q}$ and the c.m. sum momentum of the two particles $\vec{P}_{12}^{\,\mathrm{cm}} = \vec{p}_1^{\,\mathrm{cm}} + \vec{p}_2^{\,\mathrm{cm}}$, two types of the longitudinal correlation functions can be constructed

$$R^+(q) = 1 + R(q, \cos\ \zeta > 0) = 1 + R(q, v_{L,1} > v_{L,2})\,, \tag{4}$$

$$R^-(q) = 1 + R(q, \cos\ \zeta < 0) = 1 + R(q, v_{L,1} < v_{L,2})\,. \tag{5}$$

They are called the forward and backward correlation functions, corresponding to cos $\zeta > 0$ and cos $\zeta < 0$, respectively. This condition selects pairs with the longitudinal component of the velocity v_{L} (the projection on the pair velocity $\vec{v} = \vec{p}_{12}^{\,\mathrm{cm}}/(m_1 + m_2)$) of particle 1 being larger, respectively smaller than the corresponding value for particle 2. Details can be obtained from Ref. [15]. The results discussed in Ref. [15] have been obtained without any condition on the transversal momenta of the pair. For the p-d pair, the two longitudinal correlation functions are shown in Fig. 12, upper plot.

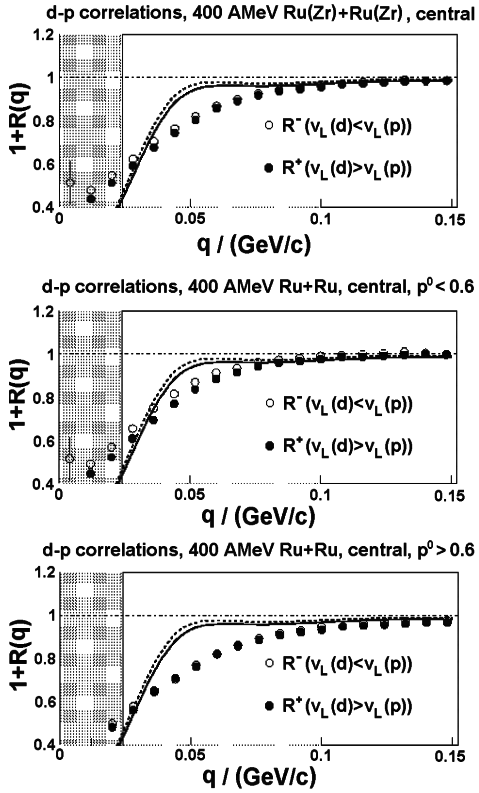

Fig. 12. Forward (full dots) and backward (open dots) longitudinal experimental correlation functions of p - d *pairs, upper plot - integrated on P° values, middle plot - P° <0.6 and lower plot - P° >0.6. The lines represent the model predictions [15].*

Triggered by the model predictions presented in Sect. 1, the same type of analysis was done but with a condition on the transverse momentum of the corresponding pair [29]. The results are presented in Fig. 12, middle and lower panels. One can observe that for $P^\circ < 0.6$, a clear difference between forward and backward longitudinal correlation functions is evidenced, while for $P^\circ > 0.6$, the two correlation functions overlap each other. Pairs in which deuterons have lower velocities (later emission time) than protons (earlier emission time) are enhanced for $P^\circ < 0.6$.

This effect can be easier followed if one represents the ratio of the forward/backward experimental correlation functions. The results can be seen in Fig. 13.

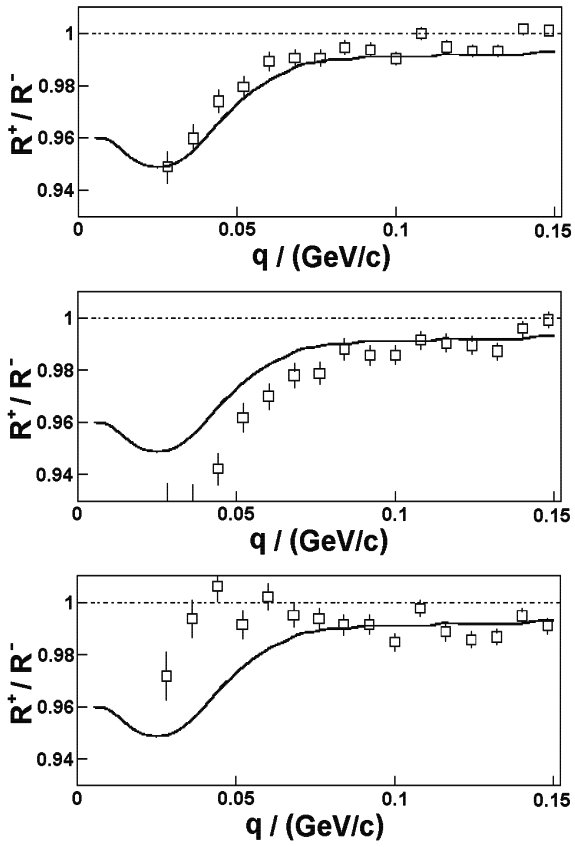

Fig. 13. Ratio of the forward/backward experimental correlation functions of p - d *pairs (open squares), upper plot - integrated on P° values, middle plot - P° <0.6 and lower plot - P° >0.6. The lines correspond to the model predictions [15].*

These experimental findings confirm the conclusions in Sect. 2, based on the hybrid model estimates that heavier fragments are produced on the average at larger values of the break-up time relative to the light particles. For $p_t^{(0)} > 0.8$, for

most products, the maximum of the distribution is localized at the same value of t_b.

For mid-central collisions, we concentrate on two experimental findings:

i) The incident energy at which the azimuthal distributions in semi-central heavy-ion collisions change from in-plane to out-of-plane enhancement, $E_{\rm tran}$, was studied recently as a function of mass of emitted particles, their transverse momentum and centrality for Au+Au [30]. A systematic decrease of $E_{\rm tran}$ as a function of mass of the reaction products and their transverse momentum was evidenced. The results are presented in Fig. 14 for CM2 centrality bin 6 fm $\leq b \leq$ 8 fm. A continuous decrease of the $E_{\rm tran}$ as a function of $p_t^{(0)}$ is evidenced for all analyzed particles, and the difference in $E_{\rm tran}$ values for different particles is decreasing towards larger values of $p_t^{(0)}$.

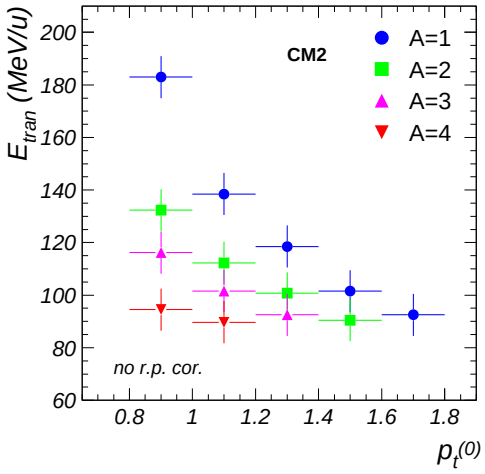

Fig. 14. The transition energy as a function of the scaled momentum for different particle types for CM2 centrality bin, for Au + Au *collision.*

For a rotating emitting source, one would expect a larger in-plane alignment for heavier fragments [31]. This effect alone can not explain the mass dependence of $E_{\rm tran}$. Therefore, a dynamical effect has to be considered besides the pure geometrical one of shadowing. Different particles, originating from different regions of the fireball, would feel the shadowing in a different way. At large $p_t^{(0)}$, the contribution comes from larger expansion velocities, earlier expansion phase of the fireball and consequently higher shadowing. At lower values of $p_t^{(0)}$, the light particles are emitted earlier, being in larger extent affected by the rotation of the fireball. Heavier fragments are emitted later, when most of the fireballs angular momentum was removed by light particle emission, and evidence stronger squeeze-out pattern. It is obvious that other effects, like preequilibrium emission, temperature smearing and sequential emission, also play a role. However, the main trends observed in the experiment confirm the expectations based on model results presented in the previous sections.

ii)The large phase-space coverage of Phase II of FOPI detector at GSI–Darmstadt SIS, allowed an extension of the studies on the participant-zone dynamics from central to mid-central heavy-ion collisions. Detailed studies of azimuthal dependence of the mean fragment and flow energies, for the Au+Au and Xe+CsI systems have been recently reported [26, 27].

Experimental mean kinetic energy values were extracted for different reaction products based on measured complete energy spectra. Their dependence as a function of reaction-product masses were fit using Eq. 1, extracting in this way the collective energy and "temperature" free of any model interpretation. This was done as a function of azimuth in a reference frame with the polar axis along the sidewards flow direction, within a polar angular range of $80° \leq \theta_{\rm cm} \leq 100°$. As an example, Fig. 15 shows the collective energy and "temperature" azimuthal distributions for two centralities, CM3 (4 – 6 fm) and ER4 (2 – 4 fm).

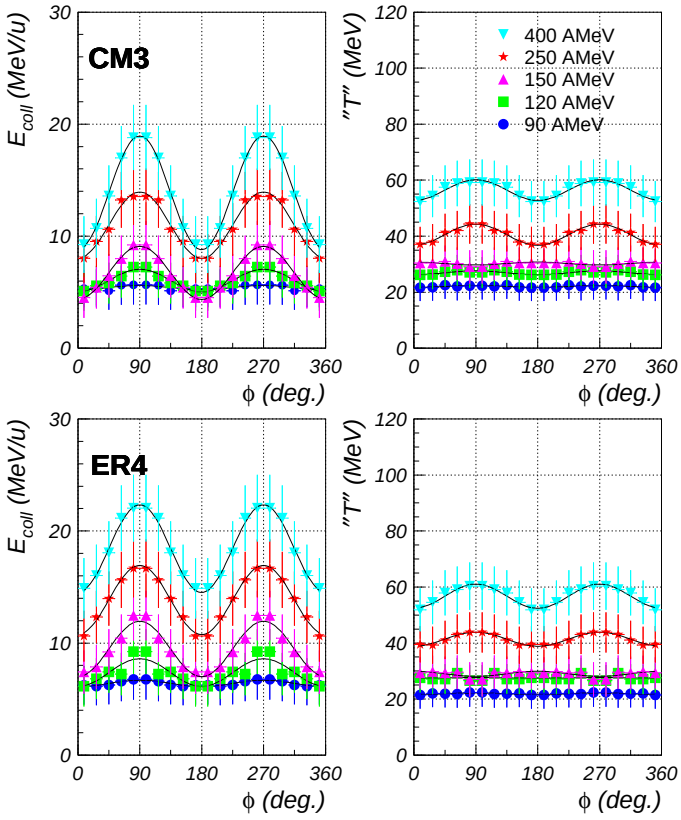

Fig. 15. Azimuthal dependence of the collective energy, $E_{\rm coll}$ and temperature "T" for Au + Au *collision at 250 A* MeV *for CM3 and ER4 centrality.*

$E_{\rm coll}$ exhibits a strong elliptic anisotropy, with the largest values in the direction perpendicular to the reaction plane, qualitatively in a good agreement with the

model predictions (see Fig. 11). This confirms that the flow energy values could be viewed as snapshots of the fireball expansion dynamics with different exposure times for different azimuthal directions.

Regarding the temperature parameter "T", it shows less significant oscillations. This could reflect the low variations of temperatures at different sides of the participant fireball [7] relative to the collective flow.

5. *Conclusions*

Model predictions on the yield distributions for different reaction products and on the collective energy of the expanding fireball, as functions of the break-up time, have been studied.

Large differences in the production yields as functions of the break-up time between different species appear in the region of low transverse momenta, heavier fragments being produced on the average at larger values of the break-up time relative to the light particles. For $p_t^{(0)} > 0.8$, for most products, the maximum of the distribution is localized at the same value of t_b.

Evidence is found for the possibility to access detailed information on the expansion process as a function of time, performing experimental studies on the azimuthal distribution of mean kinetic and collective energies for mid-central collisions.

Experimental results presented in Sect. 4 on small angle correlation functions, transition energy and azimuthal distributions of collective energy strongly support the model predictions on the possibility of extraction of detailed information on the dynamics of the fireball expansion. Therefore, we consider such observables to be sensitive probes for studying the equation of state of nuclear matter. Comparisons with the predictions of microscopic transport models, in which the symmetry term, momentum-dependent mean fields, in-medium cross sections and production of light fragments are treated in a consistent manner, could give unambiguous answer concerning the equation of state of nuclear matter.

Acknowledgements

I would like to thank all members of the FOPI collaboration at SIS/GSI for their work on which the experimental results presented in this article are based, in particular to A. Andronic, N. Herrmann, K. Hildenbrand, R. Kotte, I. Legrand, Y. Leifels, D. Pelte and G. Stoicea for numerous discussions related to the topics presented in this work. I acknowledge valuable discussions with P. Danielewicz and Peter Braun-Munzinger.

References

1) G. F. Chapline et al., Phys. Rev. D **8** (1973) 4302.
2) W. Scheid et al., Phys. Rev. Lett. **32** (1974) 741.
3) H. W. Barz et al., Nucl. Phys. A **531** (1991) 453.

4) W. Bauer et al., Phys. Rev. C **47** (1994) R1838.
5) S. C. Jeong and FOPI Collaboration, Phys. Rev. Lett. **72** (1994) 3468.
6) W. C. Hsi et al., Phys. Rev. Lett. **73** (1994) 3367.
7) M. Petrovici and FOPI Collaboration, Phys. Rev. Lett. **74** (1995) 5001.
8) G. Poggi and FOPI Collaboration, Nucl. Phys. A **586** (1995) 755.
9) M. A. Lisa et al., Phys. Rev. Lett. **75** (1995) 2662.
10) P. Braun-Munzinger et al., Phys. Lett. B **344** (1995) 43.
11) W. Reisdorf and FOPI Collaboration, Nucl. Phys. A **612** (1997) 493.
12) M. Petrovici and FOPI Collaboration, *Proc. Int. Research Workshop on Heavy Ion Physics at Low, Intermediate and Relativistic Energies using 4π Detectors*, World Scientific (1997) p. 216.
13) M. Petrovici and FOPI Collaboration, 7^{th} *Int. Conf. Clustering Aspects of Nuclear Structure and Dynamics*, World Scientific (2000) p. 337.
14) M. Petrovici and FOPI Collaboration, *Advances in Nuclear Physics*, World Scientific (2000) p. 242.
15) R. Kotte and FOPI Collaboration, Eur. Phys. J. A **6** (1999) 185.
16) H. Stöcker et al., Phys. Rev. C **25** (1982) 1873.
17) H. H. Gutbrod et al., Phys. Lett. B **216** (1989) 267.
18) M. Demoulins et al., Phys. Lett. B **241** (1989) 490.
19) D. Brill et al., Phys. Rev. Lett. **71** (1993) 336.,
20) L. B. Venema et al., Phys. Rev. Lett. **71** (1993) 835.
21) Y. Leifels et al., Phys. Rev. Lett. **71** (1993) 963.
22) D. Lambrecht et al., Z. Phys. A **350** (1994) 115.
23) S. Wang et al., Phys. Rev. Lett. **76** (1996) 3911.
24) N. Bastid and FOPI Collaboration, Nucl. Phys. A **622** (1997) 573.
25) Y. Shin et al., Phys. Rev. Lett. **81** (1998) 1576.
26) G. Stoicea and FOPI Collaboration, Phys. Rev. Lett. **92** (2004) 072303.
27) G. Stoicea, PhD Thesis, 2003
28) J. P. Bondorf et al., Nucl. Phys. A **296** (1978) 320.
29) R. Kotte, private communication, will be published
30) A. Andronic and FOPI Collaboration, Nucl. Phys. A **679** (2001) 765.
31) W. K. Wilson et al., Phys. Rev. C **51** (1995) 3136.

KAKO ISPITATI DINAMIKU ŠIRENJA VATRENE LOPTE ?

Predviđanja modela o raspodjelama prinosa za različite izlazne čestice i za skupnu energiju vatrene lopte koja se širi, koja potkrijepljuju ishodi mjerenja uzdužnih dvočestičnih korelacijskih funkcija na malim kutovima, ovisnost prijelazne energije o poprečnom impulsu, te azimutalne raspodjele skupnog širenja, jasno pokazuju na mogućnost razlučivanja različitih vremenskih intervala u dinamici vatrene lopte.